Centre for Archaeology Report 93/2001

Kwik Save, 49-53, Commercial Road, Hereford, Herefordshire: Archaeomagnetic Dating Report 2001

Paul Linford

ISSN 1473-9224

The Centre for Archaeology Reports Series incorporates the former Ancient Monuments Laboratory Report Series. Copies of Ancient Monuments Laboratory Reports will continue to be available from the Centre for Archaeology (see back of cover for details).

Centre for Archaeology Report 93/2001

Kwik Save, 49-53, Commercial Road, Hereford, Herefordshire: Archaeomagnetic Dating Report 2001

Paul Linford

Summary

A stone lined flue feature incorporating a broken quern stone was discovered by Archenfield Archaeology during evaluation excavations at 49-53, Commercial Road, Hereford. The feature possibly has parallels with a medieval corn dryer found previously in Hereford, which reused Roman masonry in its construction. Archaeomagnetic analysis of heated clay from the floor of the flue indicated that it had not been subjected to particularly intense heat during its operation. Nevertheless, it was possible to obtain a mean thermoremanent direction of magnetisation for the feature with sufficient precision to infer a date range. This direction corresponded to a magnetic pole position that has occurred more than once in the last 2000 years. Hence two possible archaeomagnetic date ranges can be inferred, one in the 3rd century AD, the other in the late 13th century AD. Archaeological evidence suggests that the former range would be extremely unlikely.

Keywords

Archaeomagnetism

Author's address
Centre for Archaeology, Fort Cumberland, Fort Cumberland Road, Eastney, Portsmouth, PO4 9LD

KWIK SAVE, 49-53, COMMERCIAL ROAD, HEREFORD, Herefordshire: Archaeomagnetic Dating Report 2001

Introduction

A stone lined flue feature was discovered by Archenfield Archaeology during an evaluation excavation prior to redevelopment of the site of the Kwik Save supermarket at 49-53, Commercial Road, Hereford (SO 515 240, Longitude 2.7°W, Latitude 52.1°N). The feature lay at the edge of a trench dug through a concrete floor and it was not immediately clear what type of structure the flue fed. The feature was unusual as it incorporated part of a (possibly Roman) quern stone as part of the stone lining of the floor of the flue. A possible parallel has previously been noted in Hereford where a similar feature was found which reused Roman masonry in its construction.

The feature was sampled for archaeomagnetic analysis by the author on the 14th of September 2001. Subsequent measurement and evaluation was also performed by the author.

Method

Samples were collected using the disc method (see appendix, section 1a) and orientated to magnetic north using a compass owing to restrictions on lines of sight into the confined excavation where the feature was situated. The deviation between magnetic north and true north was established on-site using a gyro-theodolite with built-in compass.

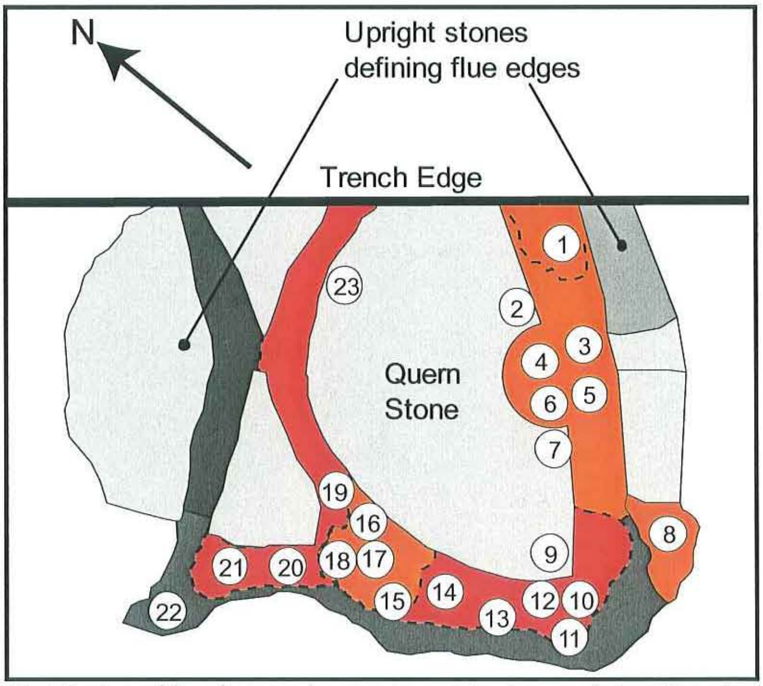

Figure 1; Sketch plan of flue feature showing approximate sample locations (not to scale).

In all, nineteen samples were collected from the clay floor of the flue surrounding the quern stone (context 47). A further four sample disks were attached to the quern stone itself, in anticipation of the possibility that subsequent archaeomagnetic analysis of it could improve the dating of the feature. The approximate locations of the samples are indicated in Figure 1. Sample 8 was taken from a small surviving piece of what appeared to be a wattle and daub superstructure that must have covered the feature that the flue fed; it was composed of orange clay. Sample 22 was taken from blackened material at the edge of the flue. All the other samples were composed of orange or orange/red, heated clay.

The natural remanent magnetisation (NRM) measured in archaeomagnetic samples is assumed to be caused by thermoremanent magnetisation (TRM) created at the time when the feature of which they were part was last fired. However, a secondary component acquired in later geomagnetic fields can also be present, caused by diagenesis or partial reheating. Additionally, the primary TRM may be overprinted by a viscous component, depending on the grain size distribution within the magnetic material. These secondary components are usually of lower stability than the primary TRM and can thus be removed by partial demagnetisation of the samples.

A typical strategy for analysing a set archaeomagnetic samples from a fired archaeological feature is to first measure their NRM magnetisation. These NRM measurements are then inspected and one or more samples are selected for pilot partial demagnetisation. Pilot demagnetisation of a sample involves exposing it to an alternating magnetic field of fixed peak strength and measuring the resulting changes in its magnetisation. The procedure is repeated with increasing peak field strengths to build up a complete picture of the coercivity spectrum of the pilot sample. From these pilot partial demagnetisation results an optimum peak field strength is selected to be applied to the remaining samples. This optimum field strength is selected to remove as much of the secondary magnetisation as possible whilst leaving the primary magnetisation intact. The equipment used for these measurements is described in section 2 of the appendix.

A mean TRM direction is then calculated from the partially demagnetised sample measurements. Some samples may be excluded from this calculation if their TRM directions are so anomalous as to make them statistical outliers from the overall TRM distribution. A "magnetic refraction" correction is often applied to the sample mean TRM direction to compensate for distortion of the earth's magnetic field due to the geometry of the magnetic fabric of the feature itself. Then the mean is adjusted according to the location of the feature relative to a notional central point in the UK (Meriden), so that it can be compared with UK archaeomagnetic calibration data to produce a date of last firing for the feature. Notes concerning the mean calculation and subsequent calibration can be found in sections 3 and 4 of the appendix.

This measurement and calibration strategy was applied to the analysis of the samples from the Hereford Kwik Save feature. As all the samples were taken from the floor of the feature, a magnetic refraction correction of 2.4° was added to the inclinations of the mean TRM direction before calibration.

Results

Sample NRM measurements and measurements after partial demagnetisation are recorded in Table 1. Figure 2 depicts the distribution of the sample TRM directions before and after partial demagnetisation. Tables 2, 3 and 4 record the pilot demagnetisation measurements made on samples 04, 08, 10, 14, 15, 18, 20 and 22. Figures 3-6 graphically illustrate these results for the measurements made on samples 04, 08, 15 and 22 respectively.

Pilot demagnetisation of sample 04 indicates that the magnetisation of this sample is relatively stable, although with a high proportion of the magnetisation being held in low coercivity domains. The other pilot demagnetisation samples all exhibit far less stability and it is likely that they have not been exposed to a temperature above the blocking temperature of titanomagnetite (580°C). Thus the flue was probably not used to channel particularly intense heat. Magnetic susceptibility measurements made on site combined with the pilot demagnetisation of sample 04 also suggest that heating was most intense in the area of clay occupied by samples 01-06 (see Figure 1), perhaps due to the way that hot air circulated within the feature.

As a result of the above, a relatively low AF field of 2.5mT was chosen to demagnetise the remaining samples. This was judged to be the optimal field for removing the low coercivity viscous remanent component from the samples' magnetisation whilst preserving as much as possible of the weak primary TRM. It is clear from Figure 2 that even after this treatment samples 08, 10, 11, 14, 18 and 22 have anomalous TRM directions with respect to the overall distribution. Sample 11 was a very small sample and samples 08 and 22 come from the edges of the feature. However, it is less clear why samples 10, 14 and 18 should be anomalous when their immediate neighbours are not. Differential composition or localised disturbances to the feature since firing may be suggested as possible explanations.

The mean TRM vector for the feature was calculated excluding these six samples:

At site:	**Dec = 4.2°**	**Inc = 61.1°**	**α_{95} = 2.9°**	**k = 208.4**
At Meriden:	**Dec = 4.5°**	**Inc = 61.4°**		

Figure 7 shows the comparison of this mean with the UK archaeomagnetic calibration curve depicted on a Bauer plot. Unfortunately the mean TRM vector corresponds with a pole position that has occurred several times in the last two millennia and two, equally probable, date ranges can be inferred from it:

265 AD to 290 AD or 1270 AD to 1305 AD at the 63% confidence level.
255 BC to 305 AD or 1255 AD to 1320 AD at the 95% confidence level.

Dates in the early 3rd and late 15th centuries AD are also possible at the 95% confidence level but have not been calculated as they are less probable than the above.

Conclusions

Archaeomagnetic study of heated clay samples from the floor (context 47) of the flue feature discovered at the Hereford Kwik Save indicate that they have acquired a TRM owing to heating associated with the operation of the feature. However, partial demagnetisation measurements demonstrate that, in the majority of cases, this magnetisation is not highly stable. This would suggest that the flue was not associated with a structure requiring intense heat. It would appear that the area immediately beneath the southern upright stone in the vicinity of samples 01-06 (see Figure 1) experienced the highest temperatures.

It was possible to derive a mean TRM direction from the sample measurements and this coincides with a virtual geomagnetic pole position that has occurred more than once in the last 2000 years. For this reason two possible date ranges are inferred, one in the 3rd century AD and one in the late 13th century AD. Evidence independent of the archaeomagnetic analysis is required to determine which is correct. However, pottery sherds found in a context immediately overlying the feature appear to date from the 12th to 13th century AD (Huw Sherlock *pers. comm.*). The Roman date range would thus appear to be extremely unlikely and the later medieval date range may be assumed to be the date of the last firing of the feature.

P. Linford
Archaeometry Branch,
Centre for Archaeology, English Heritage.

Date of report: 26/10/2001

Archaeomagnetic Date Summary

Archaeomagnetic ID:	**HKS**
Feature:	**Hereford Kwik Save Evaluation, context 47**
Location:	**Longitude 2.7°W, Latitude 52.1°N**
Number of Samples (taken/used in mean):	**19/13**
AF Demagnetisation Applied:	**2.5mT**
Distortion Correction Applied:	**+2.4°**
Declination (at Meriden):	**4.2° (4.5°)**
Inclination (at Meriden):	**61.1° (61.4°)**
Alpha-95:	**2.9°**
k:	**208.4**
Date range (63% confidence):	**265 AD to 290 AD or 1270 AD to 1305 AD**
Date range (95% confidence):	**255 BC to 305 AD or 1255 AD to 1320 AD**

		NRM Measurements				After Partial Demagnetisation			
Sample	Material	Dec°	Inc°	J(mAm^{-1})	AF(mT)	Dec°	Inc°	J(mAm^{-1})	R
HKS01	Clay	3.7	63.4	112.0	2.5	9.4	63.7	89.3	
HKS03	Clay	0.3	53.3	31.2	2.5	3.8	50.4	24.7	
HKS04	Clay	7.2	60.0	420.1	2.5	7.0	59.3	333.6	
HKS05	Clay	6.9	61.0	36.3	2.5	7.0	58.1	30.2	
HKS06	Clay	9.6	56.6	45.0	2.5	17.7	56.7	36.0	
HKS08	Clay	-19.4	66.3	249.1	2.5	-21.1	65.1	185.2	R
HKS10	Clay	39.8	74.1	80.5	2.5	42.4	73.7	67.5	R
HKS11	Clay	6.1	75.9	22.8	2.5	116.5	70.2	15.0	R
HKS12	Clay	5.2	60.5	166.4	2.5	-0.7	54.4	121.0	
HKS13	Clay	0.6	69.2	16.5	2.5	16.4	66.0	16.2	
HKS14	Clay	-39.5	38.6	80.9	2.5	-42.2	33.5	67.8	R
HKS15	Clay	-13.4	65.5	39.0	2.5	-4.4	61.0	34.4	
HKS16	Clay	9.4	59.8	55.6	2.5	8.0	58.4	44.4	
HKS17	Clay	-1.4	56.1	64.4	2.5	-0.2	54.9	50.4	
HKS18	Clay	-31.2	33.2	170.6	2.5	-27.1	29.6	142.7	R
HKS19	Clay	2.5	62.9	46.9	2.5	4.3	62.8	39.3	
HKS20	Clay	-12.7	62.0	144.4	2.5	-10.6	57.5	123.5	
HKS21	Clay	1.7	59.9	119.9	2.5	0.9	56.9	105.4	
HKS22	Clay	-40.2	57.6	317.3	2.5	-40.6	55.9	309.7	R

Table 1: Sample NRM measurements and measurements after partial AF demagnetisation for feature HKS. J = magnitude of magnetisation vector; AF = peak alternating field strength of demagnetising field; R = sample rejected from mean calculation.

	HKS04			HKS08			HKS10		
AF(mT)	Dec°	Inc°	J(mAm^{-1})	Dec°	Inc°	J(mAm^{-1})	Dec°	Inc°	J(mAm^{-1})
0.0	4.6	60.4	418.6	-19.2	66.2	249.3	40.1	73.9	83.1
2.5	7.0	59.3	333.6	-21.1	65.1	185.2	42.4	73.7	67.5
5.0	6.8	59.5	258.0	-29.4	65.2	136.1	52.0	68.8	58.3
10.0	9.0	59.5	157.7	-35.2	65.2	90.7	47.7	61.0	38.9
15.0	11.7	60.6	103.0	-31.8	64.0	70.0	39.0	53.5	27.1
20.0	14.6	58.9	75.4	-29.0	62.7	58.5	35.2	51.7	20.7
30.0	19.0	58.3	51.7	-19.5	62.5	45.7	30.1	48.3	16.6
50.0	12.1	58.3	28.9	-18.7	59.1	29.9	19.0	42.1	11.7
100.0	20.7	47.8	15.3	-17.5	44.6	11.4	13.7	54.2	5.5

Table 2: Incremental partial demagnetisation measurements for samples HKS04, HKS08 and HKS10.

	HKS14			HKS15			HKS18		
AF(mT)	Dec°	Inc°	J(mAm^{-1})	Dec°	Inc°	J(mAm^{-1})	Dec°	Inc°	J(mAm^{-1})
0.0	-38.2	38.6	82.4	-5.5	64.6	43.2	-28.5	34.0	174.9
2.5	-42.2	33.5	67.8	-4.4	61.0	34.4	-27.1	29.6	142.7
5.0	-44.6	30.6	58.2	-4.8	59.9	26.4	-23.6	30.8	108.1
10.0	-43.4	29.3	43.7	-12.9	61.9	14.4	-23.8	26.0	63.5
15.0	-42.2	29.5	34.0	-9.3	63.9	11.5	-20.5	25.6	42.3
20.0	-37.8	30.7	27.7	-7.6	61.3	9.6	-15.1	33.0	30.7
30.0	-38.1	32.0	21.5	3.7	55.2	6.8	9.5	49.1	22.3
40.0	-	-	-	-	-	-	34.4	61.7	18.9
50.0	-36.5	35.2	9.7	28.3	59.3	4.2	39.7	51.2	12.6
100.0	62.3	44.9	0.7	-	-	-	-5.0	38.9	4.9

Table 3: Incremental partial demagnetisation measurements for samples HKS14, HKS15 and HKS18.

	HKS20			HKS22		
AF(mT)	Dec°	Inc°	J(mAm^{-1})	Dec°	Inc°	J(mAm^{-1})
0.0	-12.6	59.8	147.7	-40.2	56.5	323.5
2.5	-10.6	57.5	123.5	-40.6	55.9	309.7
5.0	-9.5	57.5	103.0	-42.2	55.0	285.7
10.0	-6.8	57.2	73.3	-49.5	52.8	209.9
15.0	-4.0	58.1	55.8	-52.4	48.6	132.5
20.0	-3.7	59.6	46.0	-55.1	47.3	88.3
30.0	-3.2	57.6	37.1	-56.1	44.6	52.0
50.0	3.7	61.8	25.8	-52.0	49.4	26.3
75.0	2.8	64.6	21.4	-	-	-
100.0	0.4	62.4	18.9	-33.4	39.0	14.4

Table 4: Incremental partial demagnetisation measurements for samples HKS20 and HKS22.

Appendix: Standard Procedures for Sampling and Measurement

1) Sampling

One of three sampling techniques is employed depending on the consistency of the material (Clark, Tarling and Noel 1988):

a) **Consolidated materials:** Rock and fired clay samples are collected by the disc method. Several small levelled plastic discs are glued to the feature, marked with an orientation line related to True North, then removed with a small piece of the material attached.

b) **Unconsolidated materials:** Sediments are collected by the tube method. Small pillars of the material are carved out from a prepared platform, then encapsulated in levelled plastic tubes using plaster of Paris. The orientation line is then marked on top of the plaster.

c) **Plastic materials:** Waterlogged clays and muds are sampled in a similar manner to method 1b) above; however, the levelled plastic tubes are pressed directly into the material to be sampled.

2) Physical Analysis

a) Magnetic remanences are measured using a slow speed spinner fluxgate magnetometer (Molyneux et al. 1972; see also Tarling 1983, p84; Thompson and Oldfield 1986, p52).

b) Partial demagnetisation is achieved using the alternating magnetic field method (As 1967; Creer 1959; see also Tarling 1983, p91; Thompson and Oldfield 1986, p59), to remove viscous magnetic components if necessary. Demagnetising fields are measured in milli-Tesla (mT), figures quoted being for the peak value of the field.

3) Remanent Field Direction

a) The remanent field direction of a sample is expressed as two angles, declination (Dec) and inclination (Inc), both quoted in degrees. Declination represents the bearing of the field relative to true north, angles to the east being positive; inclination represents the angle of dip of this field.

b) Aitken and Hawley (1971) have shown that the angle of inclination in measured samples is likely to be distorted owing to magnetic refraction. The phenomenon is not well understood but is known to depend on the position the samples occupied within the structure. The corrections recommended by Aitken and Hawley are applied, where appropriate, to measured inclinations, in keeping with the practise of Clark, Tarling and Noel (1988).

c) Individual remanent field directions are combined to produce the mean remanent field direction using the statistical method developed by R. A. Fisher (1953). The quantity α_{95}, "alpha-95", is quoted with mean field directions and is a measure of the precision of the determination (see Aitken 1990, p247). It is analogous to the standard error statistic for scalar quantities; hence the smaller its value, the better the precision of the date.

d) For the purposes of comparison with standardised UK calibration data, remanent field directions are adjusted to the values they would have had if the feature had been located at Meriden, a standard reference point. The adjustment is done using the method suggested by Noel (Tarling 1983, p116).

4) Calibration

a) Material less than 3000 years old is dated using the archaeomagnetic calibration curve compiled by Clark, Tarling and Noel (1988).

b) Older material is dated using the lake sediment data compiled by Turner and Thompson (1982).

c) Dates are normally given at the 63% and 95% confidence levels. However, the quality of the measurement and the estimated reliability of the calibration curve for the period in question are not taken into account, so this figure is only approximate. Owing to crossovers and contiguities in the curve, alternative dates are sometimes given. It may be possible to select the correct alternative using independent dating evidence.

d) As the thermoremanent effect is reset at each heating, all dates for fired material refer to the final heating.

e) Dates are prefixed by "cal", for consistency with the new convention for calibrated radiocarbon dates (Mook 1986).

References

Aitken, M. J. 1990. *Science-based Dating in Archaeology*. London: Longman.

Aitken, M. J. and H. N. Hawley 1971. Archaeomagnetism: evidence for magnetic refraction in kiln structures. *Archaeometry* **13**, 83-85.

As, J. A. 1967. The a.c. demagnetisation technique, in *Methods in Palaeomagnetism*, D. W. Collinson, K. M. Creer and S. K. Runcorn (eds). Amsterdam: Elsevier.

Clark, A. J., D. H. Tarling and M. Noel 1988. Developments in Archaeomagnetic Dating in Britain. *J. Arch. Sci.* **15**, 645-667.

Creer, K. M. 1959. A.C. demagnetisation of unstable Triassic Keuper Marls from S. W. England. *Geophys. J. R. Astr. Soc.* **2**, 261-275.

Fisher, R. A. 1953. Dispersion on a sphere. *Proc. R. Soc. London A* **217**, 295-305.

Molyneux, L., R. Thompson, F. Oldfield and M. E. McCallan 1972. Rapid measurement of the remanent magnetisation of long cores of sediment. *Nature* **237**, 42-43.

Mook, W. G. 1986. Recommendations/Resolutions Adopted by the Twelfth International Radiocarbon Conference. *Radiocarbon* **28**, M. Stuiver and S. Kra (eds), 799.

Tarling, D. H. 1983. *Palaeomagnetism*. London: Chapman and Hall.

Thompson, R. and F. Oldfield 1986. *Environmental Magnetism*. London: Allen and Unwin.

Turner, G. M. and R. Thompson 1982. Detransformation of the British geomagnetic secular variation record for Holocene times. *Geophys. J. R. Astr. Soc.* **70**, 789-792.

a)

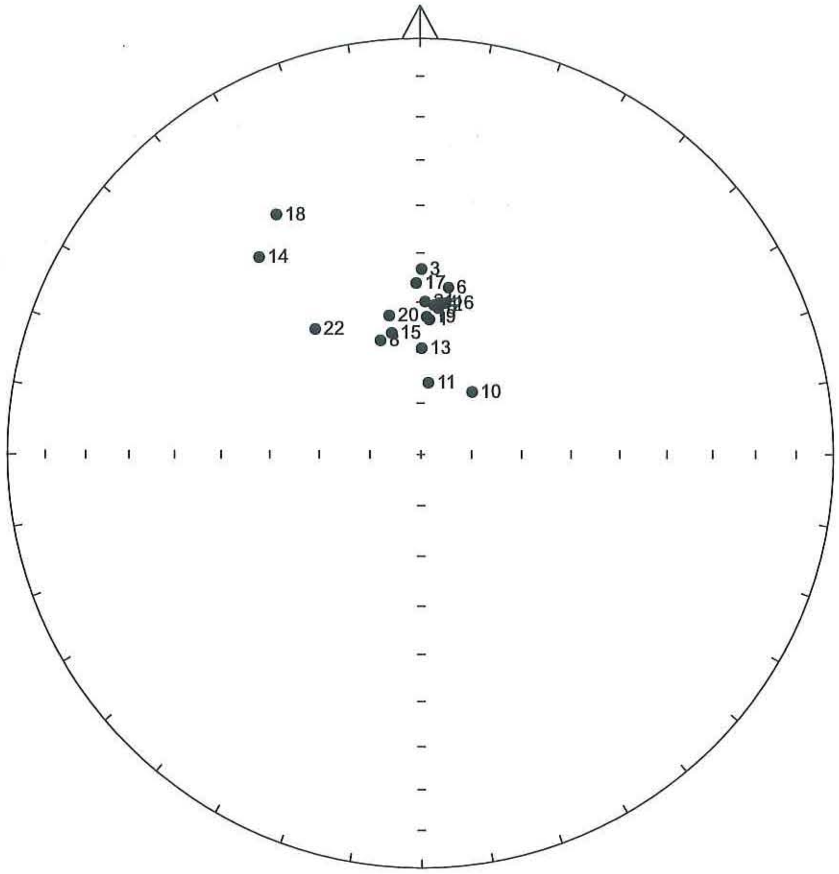

b)

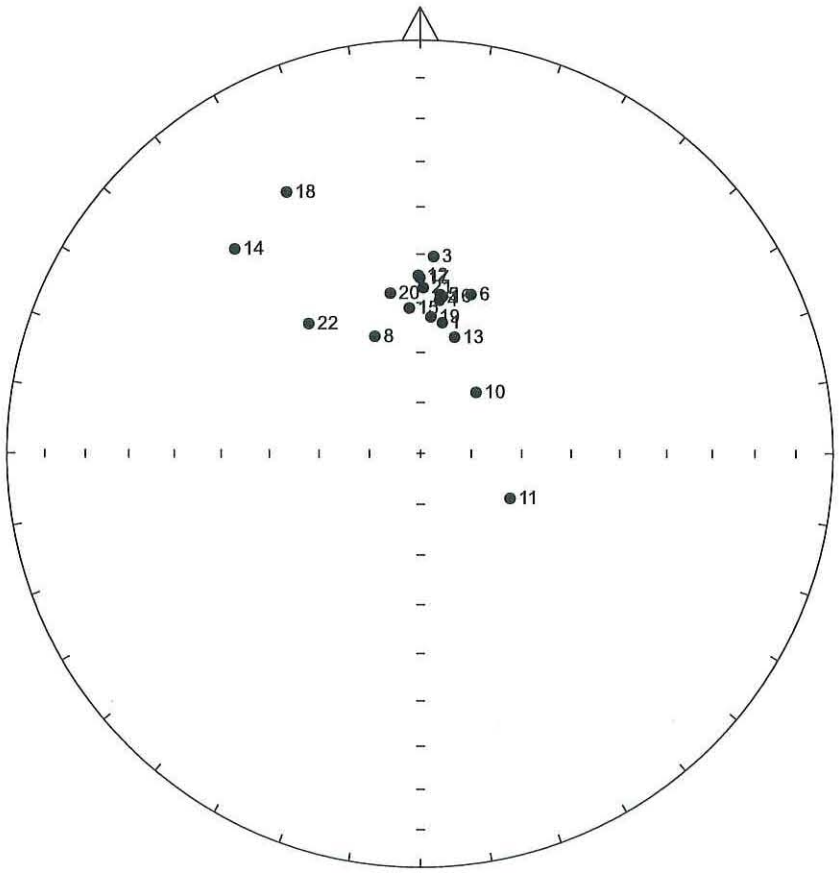

Figure 2: a) Distribution of NRM directions of samples from feature HKS represented as an equal area stereogram. In this projection declination increases clockwise with zero being at 12 o'clock while inclination increases from zero at the equator to 90 degrees in the centre of the projection. Open circles represent negative inclinations. b) Distribution of thermoremanent directions of magnetisation of the same samples after partial AF demagnetisation to 2.5mT.

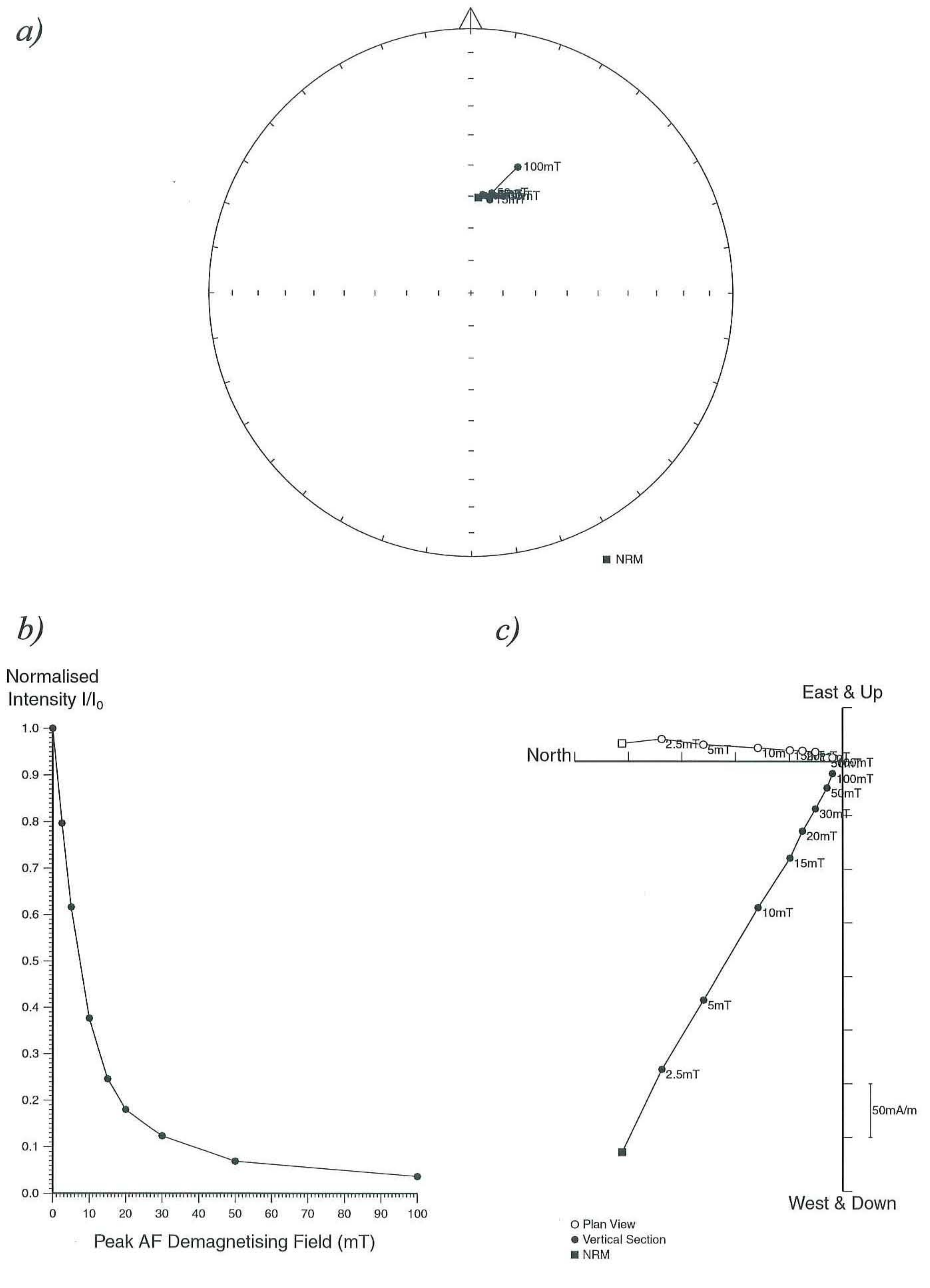

Figure 3: Stepwise AF demagnetisation of sample 04. Diagram a) depicts the variation of the remanent direction as an equal area stereogram (declination increases clockwise, while inclination increases from zero at the equator to 90 degrees at the centre of the projection); b) shows the normalised change in remanence intensity as a function of the demagnetising field; c) shows the changes in both direction and intensity as a vector endpoint projection.

a)

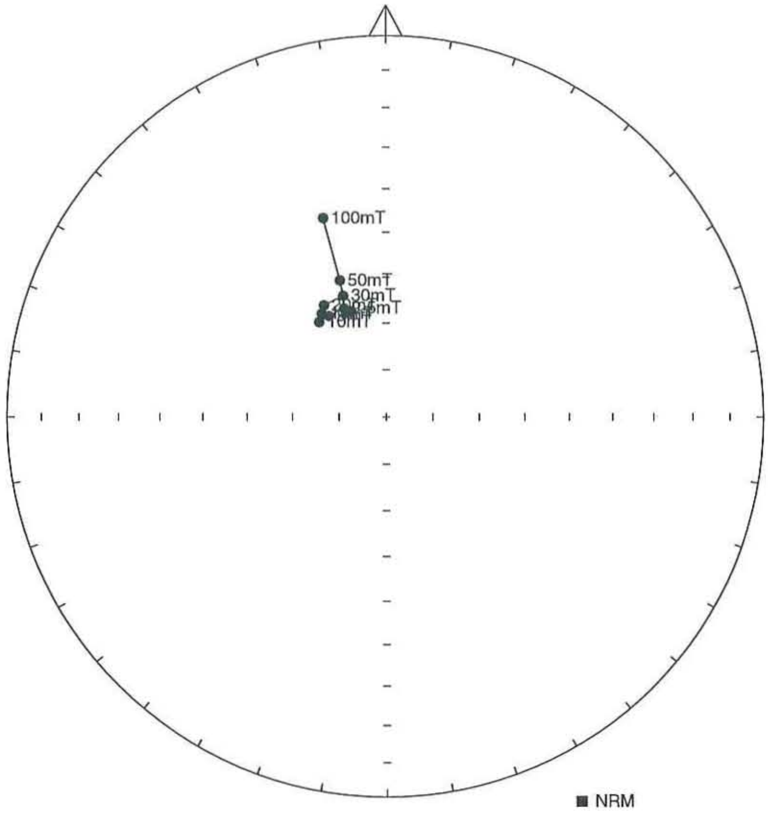

b)

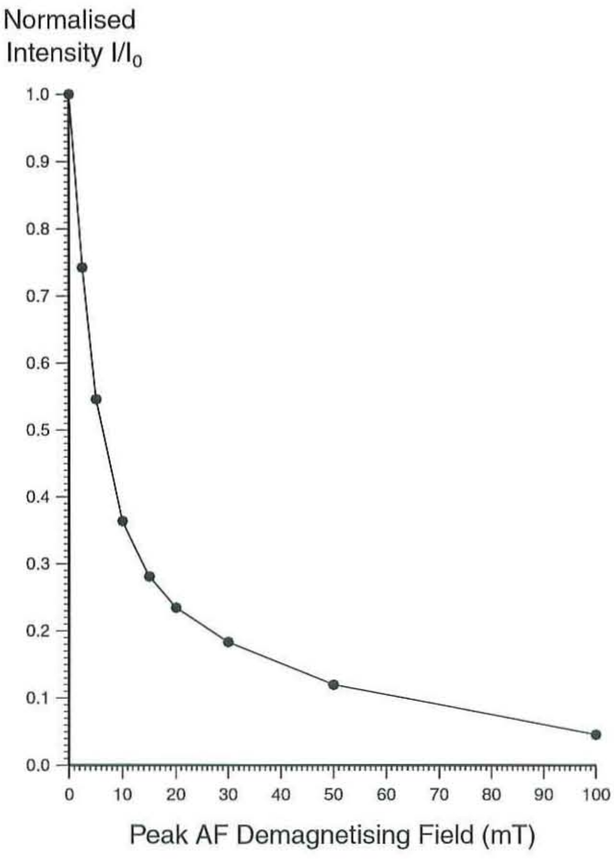

c)

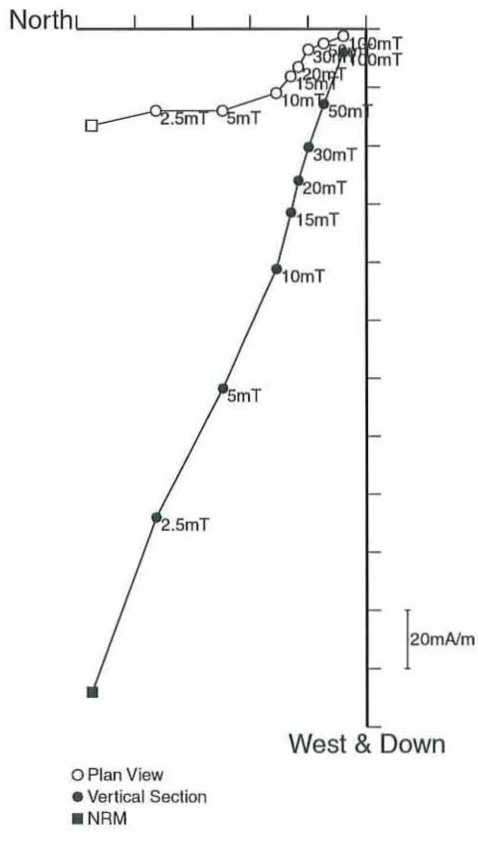

Figure 4: Stepwise AF demagnetisation of sample 08. Diagram a) depicts the variation of the remanent direction as an equal area stereogram (declination increases clockwise, while inclination increases from zero at the equator to 90 degrees at the centre of the projection); b) shows the normalised change in remanence intensity as a function of the demagnetising field; c) shows the changes in both direction and intensity as a vector endpoint projection.

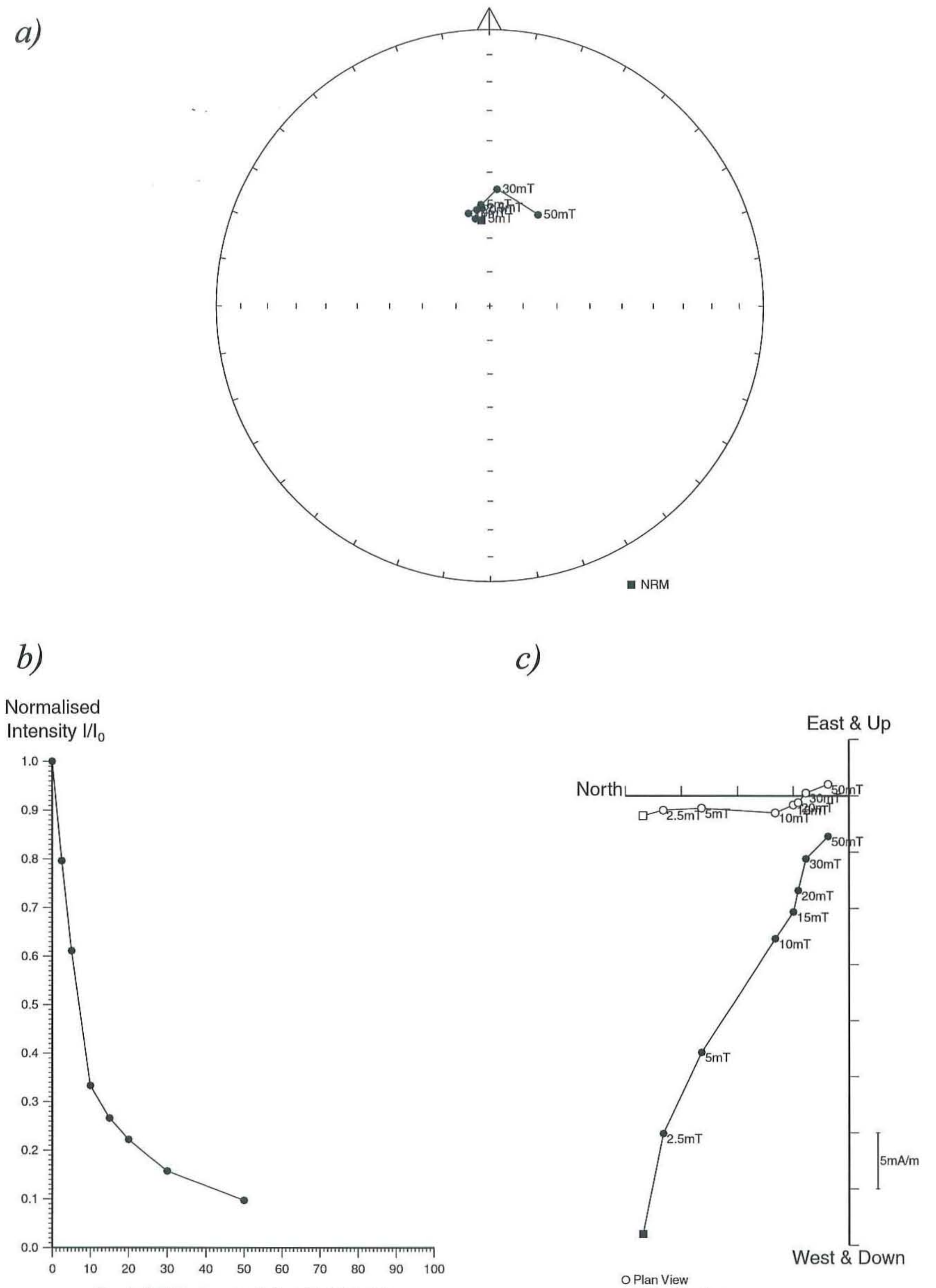

Figure 5: Stepwise AF demagnetisation of sample 15. Diagram a) depicts the variation of the remanent direction as an equal area stereogram (declination increases clockwise, while inclination increases from zero at the equator to 90 degrees at the centre of the projection); b) shows the normalised change in remanence intensity as a function of the demagnetising field; c) shows the changes in both direction and intensity as a vector endpoint projection.

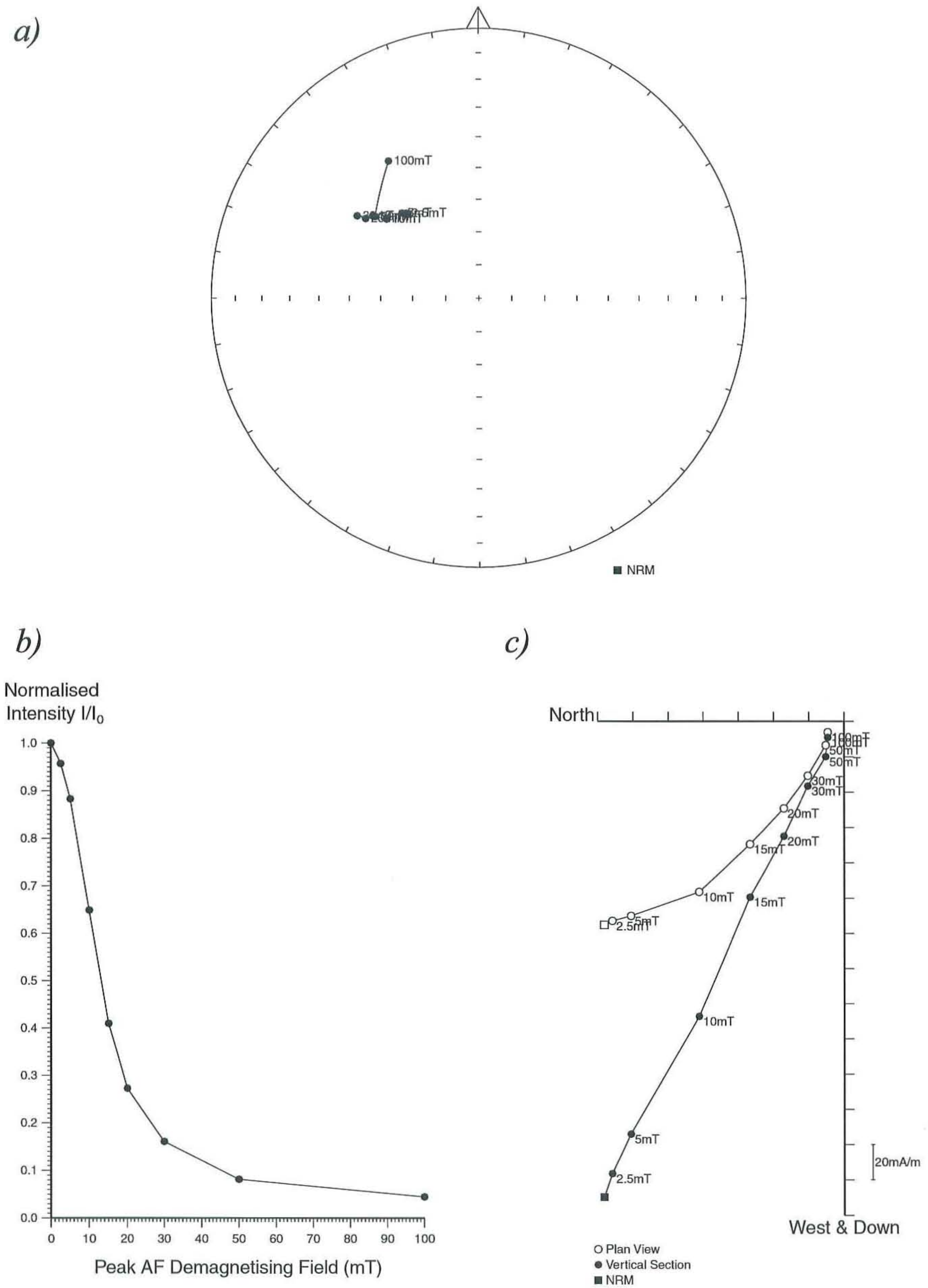

Figure 6: Stepwise AF demagnetisation of sample 22. Diagram a) depicts the variation of the remanent direction as an equal area stereogram (declination increases clockwise, while inclination increases from zero at the equator to 90 degrees at the centre of the projection); b) shows the normalised change in remanence intensity as a function of the demagnetising field; c) shows the changes in both direction and intensity as a vector endpoint projection.

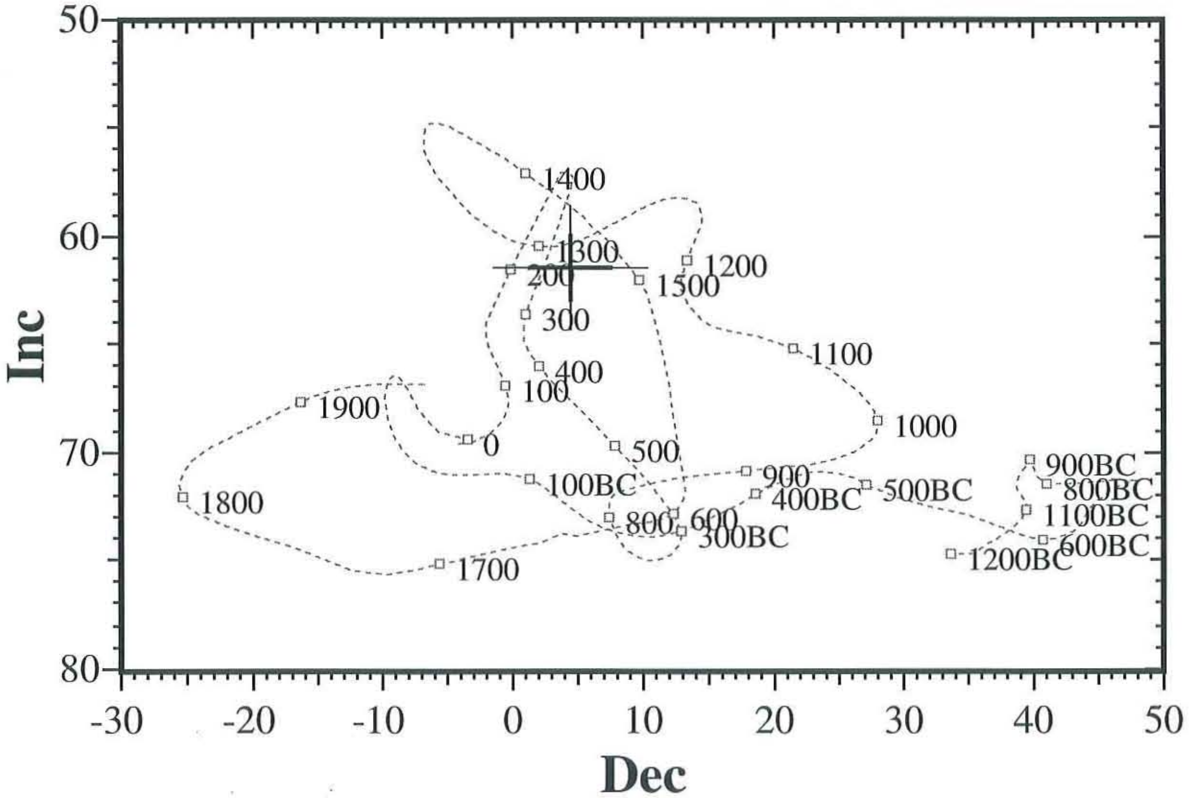

Figure 7: Comparison of the mean thermoremanent vector of samples 01, 03-6, 12-3, 15-7 and 19-21 after 2.5mT partial AF demagnetisation with the UK master calibration curve. Thick error bar lines represent 63% confidence limits and narrow lines 95% confidence limits.